Free-electron laser driven by the LBNL laser-plasma accelerator

C. B. Schroeder[*], W. M. Fawley[*], F. Grüner[†], M. Bakeman[**,*], K. Nakamura[**,*], K. E. Robinson[*], Cs. Tóth[*], E. Esarey[*,**] and W. P. Leemans[*,**]

[*]*Lawrence Berkeley National Laboratory, Berkeley, California 94720, USA*
[†]*Sektion Physik, Ludwig-Maximilians-Universität München, 85748 Garching, Germany*
[**]*University of Nevada, Reno, Nevada 89557, USA*

Abstract. A design of a compact free-electron laser (FEL), generating ultra-fast, high-peak flux, XUV pulses is presented. The FEL is driven by a high-current, 0.5 GeV electron beam from the Lawrence Berkeley National Laboratory (LBNL) laser-plasma accelerator, whose active acceleration length is only a few centimeters. The proposed ultra-fast source ($\sim$10 fs) would be intrinsically temporally synchronized to the drive laser pulse, enabling pump-probe studies in ultra-fast science. Owing to the high current ($\gtrsim$10 kA) of the laser-plasma-accelerated electron beams, saturated output fluxes are potentially greater than 10^{13} photons/pulse. Devices based both on self-amplified spontaneous emission and high-harmonic generated input seeds, to reduce undulator length and fluctuations, are considered.

Keywords: Free-electron laser, laser-plasma accelerator
PACS: 41.60.Cr, 52.38.Kd

INTRODUCTION

Recent experiments at LBNL have demonstrated generation of low energy spread, GeV beams using laser-plasma-based acceleration [1]. These experiments used a relativistically intense ($>10^{18}$ W/cm^2) laser pulse focused into a plasma channel (plasma density $\sim 10^{18}$ cm^{-3}) to generate plasma waves with accelerating fields on the order of 100 GV/m. The cm-scale plasma channels are created using a gas-filled discharge capillary. The electron bunches are self-trapped from the background plasma and have naturally short durations (a fraction of the plasma period, $\sim$10 fs). With such short durations, peak currents $\gtrsim$10 kA are generated. The ultra-short laser-plasma accelerated beams are well-suited to drive an FEL, and the ultra-high currents allow for greatly reduced undulator lengths. The bunches emerging from the laser-plasma accelerator are also intrinsically synchronized to the laser driver, making such a source ideal for ultra-fast pump-probe applications. These laser-plasma accelerator experimental results [1] open the possibility of a new class of compact, high-peak flux, FELs in which the conventional accelerator is replaced by a GeV-class laser-plasma accelerator (several cm in length), in principle greatly reducing the size and cost of such light sources [2–5].

In this paper we discuss the design of a compact free-electron laser (FEL) driven by the LBNL laser-plasma accelerator. GeV electron beams with $\sim 10^{-2}$ relative energy spread and $\sim$mrad divergences (implying $\sim$1 mm-mrad normalized emittance) contain-

TABLE 1. Undulator parameters.

Undulator type	planar
Undulator period, λ_u	2.18 cm
Peak magnetic field, B_0	1.02 T
Undulator parameter (peak), K	1.85
Magnetic gap	4.8 mm
Undulator periods, N_u	220
Beta-function, k_β^{-1}	3.7 m

ing $\sim 10^9$ electrons have been demonstrated at LBNL [1, 6]. Further improvements in beam quality (e.g., reducing the relative energy spread to $< 10^{-2}$) are anticipated using triggered electron trapping via plasma density gradients [7].

FEL DESIGN

We consider the interaction of a laser-plasma-accelerated 0.5 GeV electron beam in a conventional magnetostatic undulator. Recently, the THUNDER undulator [8] has been transported to LBNL from Boeing and, after magnetic measurements are concluded [9], is scheduled for installation in 2009. The undulator characteristics are listed in Table 1. The undulator period is 2.18 cm, and the peak undulator strength parameter is $K = eB_0\lambda_u/2\pi mc^2 \simeq 1.85$ (peak magnetic field of $B_0 \approx 1.02$ T). The undulator consists of ten, 22-period, sections, and the undulator strength may be tapered section by section. A canted pole design allows for focusing in both planes. A beta-function of 3.7 m for 0.5 GeV in both planes is accomplished by the natural focusing and the canted pole design [8]. We will assume the laser-plasma-accelerated electron beam parameters listed in Table 2. For the numerical modeling a parabolic current distribution was assumed.

The resonant fundamental wavelength for the undulator and beam parameters listed in Tables 1 and 2 is $\lambda = \lambda_u(1+K^2/2)/(2\gamma^2) \simeq 31$ nm (40 eV photons), while the matched electron beam size in the undulator is $\sigma_x = \sigma_y = 61\ \mu$m. The basic scalings of the FEL are determined by the FEL parameter:

$$\rho = \frac{1}{2\gamma}\left[\frac{I}{I_{\rm A}}\left(\frac{KF\lambda_u}{2\pi\sigma_r}\right)^2\right]^{1/3}, \qquad (1)$$

with I the peak current, $I_{\rm A} = mc^3/e \simeq 17$ kA, $\sigma_r = \sqrt{2}\sigma_x$ the beam radius, $F = [J_0(\chi) -$

TABLE 2. Laser-plasma-accelerator beam parameters.

Beam energy, γmc^2	0.5 GeV
Peak current, I	20 kA
Charge, Q	0.2 nC
Bunch duration (FWHM), τ_b	10 fs
Energy spread (RMS, slice), σ_γ/γ	0.5%
Normalized transverse emittance, ε	1 mm mrad

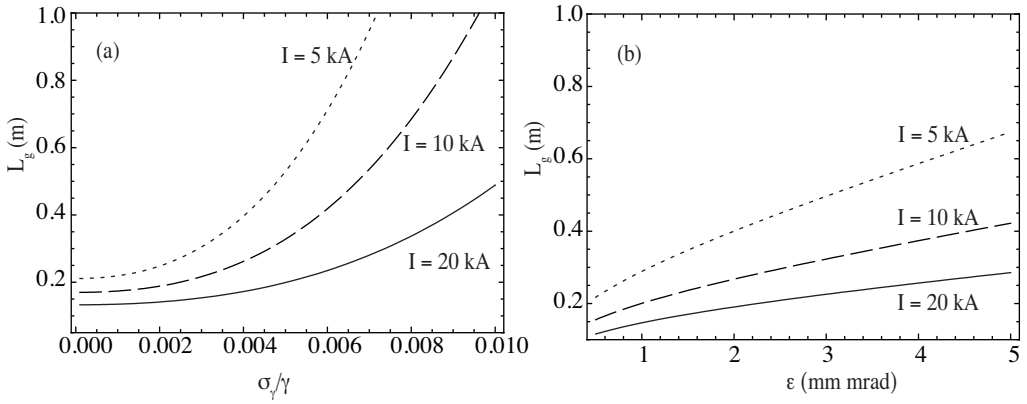

FIGURE 1. Power gain length versus (a) relative energy spread and (b) normalized transverse emittance for peak beam currents of 5 kA (dotted curve), 10 kA (dashed curve), and 20 kA (solid curve), with all other parameters are given in Tables 1 and 2.

$J_1(\chi)]$ (planar undulator), $\chi = K^2(4+2K^2)^{-1}$, and J_m are Bessel functions. For the parameters of Tables 1 and 2, the FEL parameter is $\rho \approx 8\times 10^{-3}$ and the ideal one-dimensional (i.e., neglecting emittance, energy spread, or diffraction effects) exponential power gain length is $L_{1D} = \lambda_u/(4\pi\sqrt{3}\rho) \simeq 0.12$ m. Including these non-ideal effects (emittance, energy spread, and diffraction), via the Xie gain length formula [10], the gain length increases to $L_g = 0.23$ m for the parameters of Tables 1 and 2. Figure 1 shows L_g versus (a) relative energy spread and (b) normalized transverse emittance, for several peak currents. Operating at relatively large currents (i.e., larger ρ) relaxes the electron beam quality requirements. Note that slippage will be an important effect at these energies and pulse durations. The slippage over the full THUNDER undulator is $\tau_s = \lambda N_u/c \approx 24$ fs, and operating with electron beam pulse durations τ_b below τ_s will reduce the saturated radiation power.

The saturation length of the FEL is approximately given by $L_{\rm sat} \sim \lambda_u/\rho$, and, therefore, the saturation length scales as $L_{\rm sat} \propto (I_{\rm A}/I)^{1/3}$. For the ultra-high currents of the laser plasma accelerated electron beams, $I \sim I_{\rm A}$, the saturation length is significantly reduced (compared to a beam generated from a conventional accelerator with $I \ll I_{\rm A}$). A compact FEL is enabled not only by the compact laser-plasma accelerator, but by the reduced undulator length resulting from the ultra-high peak currents of the laser-plasma accelerator electron beam.

Space charge effects will not directly affect the FEL instability in this high-current regime provided $(\lambda_u/\rho)^2 \ll \gamma^3\lambda_p^2$ (i.e., the characteristic wavelength of the space charge oscillation in the lab frame is much greater than the FEL gain length), where λ_p is the plasma wavelength of the electron beam. This condition is satisfied for the parameters of Tables 1 and 2. However, a space-charge induced energy chirp $\delta\gamma/\gamma$ is can be created by the longitudinal Coulomb self-fields during beam propagation in vacuum. The space-charge induced energy chirp $\delta\gamma/\gamma$ over a coherence length $L_c = \lambda L_g/\lambda_u$ should be small compared to the FEL bandwidth ρ. Large space-charge chirps are inhibited by growth of the longitudinal bunch length (at the % level), and the space-charge induced chirp is not expected to significantly affect the FEL performance for these parameters [11]. Resistive

TABLE 3. FEL parameters and performance.

Fundamental radiation wavelength, λ	31 nm
Resonant photon energy	40 eV
FEL parameter, ρ	0.008
3D Gain length, L_g	0.23 m
RMS bandwidth at saturation	0.005
Slippage length	7 μm
Spontaneous radiation power	16 kW
Saturation length (SASE)	5 m
Saturation length (HHG-seeded)	2.4 m
Photons/pulse (HHG-seeded)	4×10^{13}
Peak brightness* (HHG-seeded)	3×10^{16}

* photons/pulse/mm^2/mrad^2/0.1%BW

wall wakefields can also create an energy chip. For the 4.8 mm minimum undulator gap, given the ultra-short bunch durations ($\tau_b \sim 10$ fs), resistive wall wakefields will not significantly degrade the performance of the FEL for peak currents $I <$30 kA.

FEL PERFORMANCE

The simplest mode of FEL operation is to rely on self-amplified spontaneous emission (SASE) in the undulator. SASE operation allows for straightforward wavelength tuning via the beam energy or undulator gap. Owing to the intrinsic synchronization between the laser and the electron beam, it is natural to also consider external seeding by a high-harmonic generation (HHG) source at the FEL fundamental wavelength [12]. Existing laboratory HHG sources have demonstrated production of ultra-short (tens of fs) coherent pulses at 31 nm with 0.3 μJ of energy (see, for example, Ref. [13]). For the numerical modeling below, we have adopted nominal seed parameters of a Gaussian pulse with 15 MW peak intensity and a FWHM duration of 10 fs. HHG seeding has significant advantages over the simpler SASE mode of operation as it provides improved temporal coherence, reduced fluctuations, and a much reduced power saturation length. Table 3 lists the FEL parameters and performance.

Figure 2 shows the exponential gain in time-integrated radiation pulse energy over the length of the undulator for the SASE and HHG-seeded cases. These results were obtained using the `GINGER` code [14], and the SASE result is one example of start-up from shot noise (shot-to-shot fluctuations are present in this short-bunch regime $c\tau_b \sim 2\pi L_c$). For SASE, saturation is reached after approximately 5 m, and the FEL produces 10^{13} photons/pulse. Using seeding, the saturation length is approximately 2.4 m, and the power in the third harmonic(10.3 nm) is about 0.5% that of the fundamental. Earlier saturation can also be achieved by employing additional focusing (adding focusing optics between the undulator sections) to reduce the matched beam radius (increase ρ).

Figure 3 shows an example (a single `GINGER` simulation run) of the temporal structure of the radiation after the full THUNDER undulator for the SASE and the HHG cases. The dominance of a single longitudinal mode in the SASE case is due to slippage (the electron beam is centered at $t = 0$ in Fig. 3) and the fact that the ultra-short

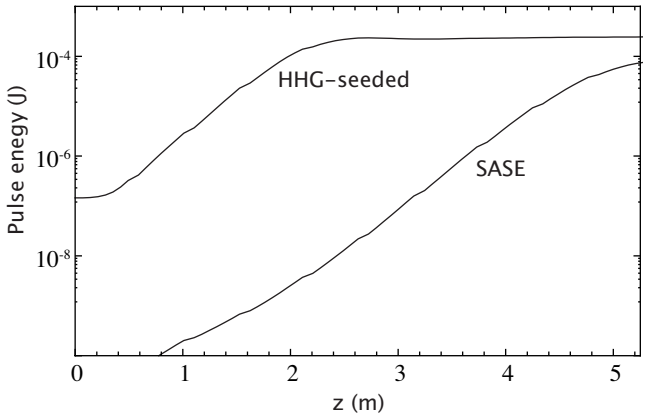

FIGURE 2. Predicted (GINGER simulation) radiation pulse energy as a function of undulator length for SASE and HHG-seeded cases.

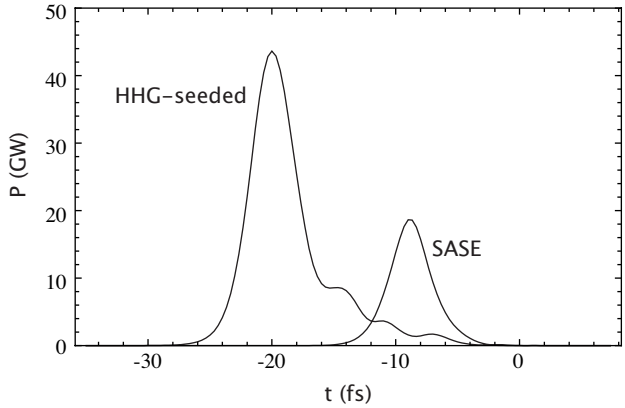

FIGURE 3. Example of temporal profiles (SASE and HHG-seeded cases) of the output FEL radiation power (GINGER simulation). The electron beam is centered at $t = 0$.

bunch duration (10 fs) is on the order of $2\pi L_c$, where the steady-state coherence length is $L_c = \lambda L_g/\lambda_u \simeq 0.3\ \mu$m. For SASE, the short bunches also result in significant shot-to-shot fluctuations in peak power.

DISCUSSION AND CONCLUSIONS

Recent advances in laser-plasma-based accelerator experiments, and, in particular, the demonstration of high-quality GeV electron beams [1, 6], have enabled the possibility of a new class of compact laser-driven FELs in which the conventional RF accelerator is replaced by a cm-scale laser-plasma accelerator that produces ultra-short (high current) GeV beams over cm-scale distances. These advances are expected to greatly reduce the size, and cost, of future FELs. The natural short bunch duration of the laser-plasma accelerated beam ($\sim$10 fs), and the intrinsic temporal synchronization between the short-pulse laser generating the electron beam and the FEL radiation, make the laser-driven

FEL an ideal source for ultra-fast pump-probe applications. For the design parameters discussed in this paper, ultra-short, coherent XUV pulses containing 10^{13} photons/pulse can be produced in $\sim$5 m. To achieve this level of performance, the energy spread of the laser-plasma accelerated electron beam must be reduced an order of magnitude (to $\lesssim 0.5\%$) compared to present experimental results. Seeding of the FEL by an HHG source (generated from the same drive laser as the plasma accelerator, and, therefore, temporally synchronized with the electron beam) can reduce the overall length of the device, as well as reducing shot-to-shot fluctuations.

ACKNOWLEDGMENTS

This work was supported by the Director, Office of Science, of the U.S. Department of Energy under Contract No. DE-AC02-05CH11231 and by NSF Contract No. 0614001 at the Univ. of Nevada, Reno. Prof. F. Grüner was supported by Deutsche Forschungsgemeinschaft through the DFG-Cluster of Excellence Munich-Centre for Advanced Photonics. We would like to express our appreciation to Boeing Phantom Works for making the THUNDER undulator available through an extended loan for these experiments. We are also grateful for Boeing's assistance in preparing shipping THUNDER to LBNL.

REFERENCES

1. W. P. Leemans, B. Nagler, A. J. Gonsalves, C. Tóth, K. Nakamura, C. G. R. Geddes, E. Esarey, C. B. Schroeder, and S. M. Hooker, *Nature Phys.* **2**, 696–699 (2006).
2. D. A. Jaroszynski, R. Bingham, E. Brunetti, B. Ersfeld, J. Gallacher, B. van der Geer, R. Issac, S. P. Jamison, D. Jones, M. de Loos, A. Lyachev, V. Pavlov, A. Reitsma, Y. Saveliev, G. Vieux, and S. M. Wiggins, *Philos. Trans. R. Soc. London, Ser. A* **364**, 689—710 (2006).
3. C. B. Schroeder, W. M. Fawley, E. Esarey, and W. P. Leemans, "DESIGN OF AN XUV FEL DRIVEN BY THE LASER-PLASMA ACCELERATOR AT THE LBNL LOASIS FACILITY," in *Proceedings of FEL 2006*, JACoW, www.JACoW.org, 2006, pp. 455–458.
4. F. Grüner, S. Becker, U. Schramm, T. Eichner, M. Fuchs, R. Weingartner, D. Habs, J. Meyer-ter-Vehn, M. Geissler, M. Ferrario, L. Serafini, B. van der Geer, H. Backe, W. Lauth, and S. Reiche, *Appl. Phys. B* **86**, 431–435 (2007).
5. K. Nakajima, *Nature Phys.* **4**, 92–93 (2008).
6. K. Nakamura, B. Nagler, C. Tóth, C. G. R. Geddes, C. B. Schroeder, E. Esarey, W. P. Leemans, A. J. Gonsalves, and S. M. Hooker, *Phys. Plasmas* **14**, 056708 (2007).
7. C. G. R. Geddes, K. Nakamura, G. R. Plateau, C. Toth, E. Cormier-Michel, E. Esarey, C. B. Schroeder, J. R. Cary, and W. P. Leemans, *Phys. Rev. Lett.* **100**, 215004 (2008).
8. K. E. Robinson, D. C. Quimby, and J. M. Slater, *IEEE J. Quantum Electron.* **QE-23**, 1497–1513 (1987).
9. M. Bakeman et al. (2008), in these Proceedings.
10. M. Xie, *Nucl. Instrum. Methods Phys. Res. A* **445**, 59–66 (2000).
11. F. J. Grüner, C. B. Schroeder, A. R. Maier, S. Becker, and Y. M. Mikhailova, *Phys. Rev. ST Accel. Beams* (submitted, 2008).
12. G. Lambert, T. Hara, D. Garzella, T. Tanikawa, M. Labat, B. Carre, H. Kitamura, T. Shintake, M. Bougeard, S. Inoue, Y. Tanaka, P. Salieres, H. Merdji, O. Chubar, O. Gobert, K. Tahara, and M. Couprie, *Nature Phys.* **4**, 296–300 (2008).
13. E. Takahashi, Y. Nabekawa, T. Otsuka, M. Obara, and K. Midorikawa, *Phys. Rev. A* **66**, 021802(R) (2002).
14. W. M. Fawley, A user manual for GINGER and its post-processor XPLOTGIN, Technical Report LBNL-49625, Lawrence Berkeley National Laboratory (2002).